

Multivalent Macromolecules Redirect Nucleation-Dependent Fibrillar Assembly into Discrete Nanostructures

Yang Song,^{†,‡} Pin-Nan Cheng,^{†,‡} Lijuan Zhu,^{†,‡} Edwin G. Moore,[†] and Jeffrey S. Moore^{*,†,‡}

[†]Department of Chemistry and [‡]Beckman Institute for Advanced Science and Technology, University of Illinois at Urbana-Champaign, Urbana, Illinois 61801, United States

S Supporting Information

ABSTRACT: Manipulating the size and shape of non-covalent multivalent assemblies is an ongoing challenge in the field of supramolecular polymers. Following a mechanistic approach, we reasoned that nucleation–elongation kinetics presents unique opportunities for controlled growth since the final outcome is likely to depend on the structure and dynamics of critical-nucleus formation. Taking fibrillar assembly of amyloid β ($A\beta$) peptide as the model system of nucleation-dependent supramolecular polymerization, here we report multivalent polymer–peptide conjugates (mPPCs) that redirect fibrillar assembly of $A\beta$ to form discrete nanostructures. The mPPCs were rationally designed to target $A\beta$ intermediates formed prior to critical nucleation. Atomic force microscopy and transmission electron microscopy studies show that in the presence of mPPCs, $A\beta$ self-assembles into zero-dimensional discrete nanostructures with lateral dimensions approximately in 5–35 nm, while $A\beta$ alone self-assembles into one-dimensional fibrils in micrometer. Thioflavin T kinetics fluorescence assays demonstrate that mPPCs suppress $A\beta$ fibrillogenesis. The mPPCs may thus represent a prototypical molecular design of multivalent macromolecules able to control the final shape of supramolecular polymers assembled via a nucleation-dependent mechanism.

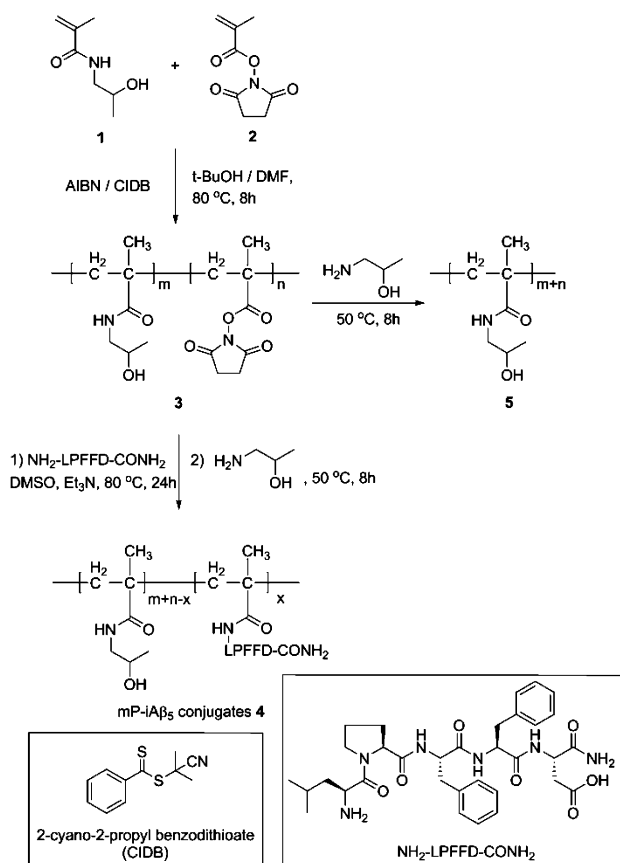
Self-assembly of fibrillar structures via nucleation-dependent mechanisms occurs ubiquitously in biological systems such as protein aggregation, and in synthetic materials such as supramolecular gels and synthetic polymers.¹ Compared to the well-studied controlled covalent polymerization, control of supramolecular polymerization to form structurally well-defined assemblies remains largely unknown and challenging.² Mechanistically, fibrillar self-assembly is a supramolecular polymerization process which consists of two phases: a slow nucleation phase followed by a rapid chain growth phase.³ During nucleation, the noncovalent interactions between monomers are weak and the initial oligomerization is energetically disfavored. Since the size and shape of the final assemblies are likely to be sensitive to both the structure of the nucleus and its kinetics of growth, we reasoned that molecular specific interactions at this stage presented an opportunity to manipulate and control the assembly process. Here we report rationally designed multivalent polymer–peptide conjugates (mPPCs) that modulate nucleation-dependent assembly of

amyloid β ($A\beta$) peptide, redirecting the formation of normal $A\beta$ fibrils into discrete nanostructures. For $A\beta$ assemblies, it is widely accepted that during the nucleation phase of aggregation, metastable prefibrillar intermediates form through hydrophobic collapse with development of β -sheet interactions between the central hydrophobic sequence $A\beta_{17-21}$ (LVFFA).⁴ Taking advantage of this nature of $A\beta$ aggregation, we designed and synthesized multivalent polymer- $iA\beta_5$ (mP- $iA\beta_5$) conjugates in which LPFFD ($iA\beta_5$) was selected as the peptide fragment for the mPPCs, given its known binding with specificity to $A\beta_{17-21}$.⁵ Thioflavin T (ThT) fluorescence assays, atomic force microscopy (AFM), and transmission electron microscopy (TEM) studies show that mP- $iA\beta_5$ conjugates effectively modulate $A\beta_{40}$ aggregation and redirect the formation of one-dimensional $A\beta$ fibrils in microscale into zero-dimensional discrete nanostructures.

The multivalent polymer–peptide conjugates were constructed by conjugating multiple copies of $A\beta$ binding peptides onto a linear copolymer backbone **3**. By controlling the stoichiometry of polymers to peptides, the polymer–peptide conjugates with different peptide loadings were synthesized to accomplish different multivalency. Poly(*N*-(2-hydroxypropyl)methacrylamide) (PHPMA) was selected as the polymeric scaffold due to its water solubility, zero net charge at neutral pH, and well-established synthesis.⁶ The synthesis started with the copolymerization of *N*-(2-hydroxypropyl)methacrylamide (HPMA) **1** and *N*-hydroxysuccinimide methacrylate (NHSMA) **2** by reversible addition–fragmentation chain transfer (RAFT) polymerization to yield poly(HPMA-*co*-NHSMA) **3** (Scheme 1).⁷ The molecular weight and polydispersity of **3** were determined by GPC (Figure S2), and the degree of polymerization was approximately 300. Peptide $iA\beta_5$ was conjugated to **3** using different stoichiometric ratios, and all remaining active ester groups were then quenched by 1-amino-2-propanol to yield mP- $iA\beta_5$ conjugates **4**.⁸ Three mP- $iA\beta_5$ conjugates were prepared having on average 3, 7, and 12 mol % of $iA\beta_5$ per polymer chain (Figures S5–S10). On the basis of the degree of polymerization, these conjugates have 9, 21, and 36 copies of $iA\beta_5$ per chain, respectively. We use the notation mP- $iA\beta_5$ -3%, mP- $iA\beta_5$ -7%, and mP- $iA\beta_5$ -12% to designate the peptide loading of these three conjugates. PHPMA polymer **5** was synthesized by quenching **3** with 1-amino-2-propanol to serve as a control for conjugates **4**.

Received: January 31, 2014

Published: March 24, 2014

Scheme 1. Synthesis of mP-iA β_5 Conjugates 4

ThT assays demonstrate that the multivalent design of mP-iA β_5 conjugates 4 leads to the enhanced activity against A β_{40} aggregation when compared to monovalent iA β_5 . In ThT assays the upturn in fluorescence follows a characteristic lag time that is extensively used to estimate the modulatory effects of inhibitors on A β aggregation.⁹ A longer lag time generally corresponds to a slower nucleation kinetics and a better modulatory effect. In the presence of 2.1 equiv of iA β_5 per A β_{40} (2.1 equiv of iA β_5 approximately equal to the amount of iA β_5 copies attached to 0.1 equiv of mP-iA β_5 -7% 4), the lag time did not significantly change when compared to that of A β_{40} control without any modulators (green and black bars in Figure 1). In contrast, mP-iA β_5 -3% conjugate 4 delayed A β_{40} aggregation by 83% at 0.1 equiv, increasing the lag time from 240 to 440 min. Moreover, mP-iA β_5 -7% 4 delayed A β_{40} aggregation by 171% at 0.1 equiv, increasing the lag time from 240 to 650 min, while mP-iA β_5 -12% 4 delayed A β_{40} aggregation by 75% at 0.1 equiv, increasing the lag time from 240 to 420 min. These results indicate that mP-iA β_5 conjugates 4 (0.1 equiv) are much more active than monovalent iA β_5 (2.1 equiv). To investigate the effect of the PHPMa polymer backbone on A β_{40} aggregation, we incubated A β_{40} in the presence of 0.1 equiv of control polymer 5 with and without 2.1 equiv of iA β_5 . Our ThT data show that both polymers control only slightly delayed A β_{40} aggregation (red and blue bars in Figure 1). Accordingly, the ThT assays confirm that the enhanced activities of conjugates 4 mainly result from the multivalent effect. In addition, ThT results indicate that higher loading of conjugates 4 do not necessarily lead to slower nucleation kinetics and better modulatory effect. Instead, mP-iA β_5 -7% 4 achieves the longest delay against A β_{40} aggregation, which suggests an optimal

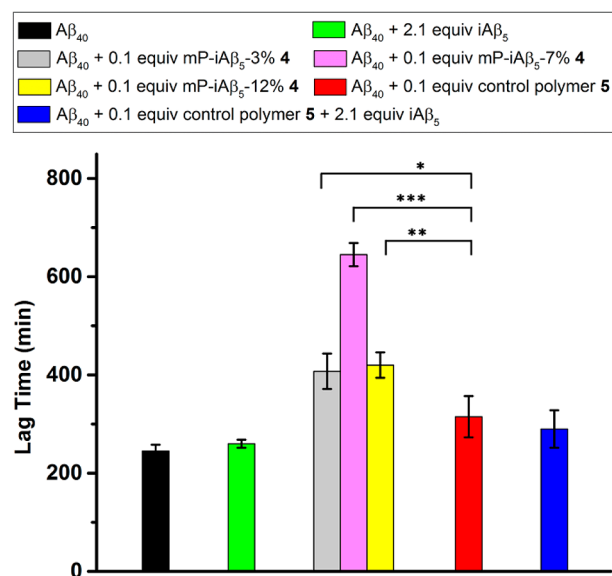


Figure 1. Modulatory effect of mP-iA β_5 conjugates 4 on A β_{40} aggregation monitored by Thioflavin T fluorescence assays. Lag time of A β_{40} aggregation in the absence or presence of mP-iA β_5 conjugates 4 (see Figures S14–S16 for ThT assays curves). A prolonged lag time is an indicator of inhibition of A β aggregation and slow nucleation kinetics. ThT assays were performed on 15 μM (1.0 equiv) A β_{40} peptide in 10 mmol PBS buffer (pH 7.4) at 37 °C with 567 rpm shaking speed. (Results from *t* test, * $p < 1 \times 10^{-3}$; ** $p < 1 \times 10^{-4}$; *** $p < 1 \times 10^{-7}$).

peptide loading (Figure 1). One possible explanation for this observation is that the peptides in mP-iA β_5 -12% 4 start to self-associate, thereby competing with their intermolecular interactions to A β_{40} .¹⁰ The above results demonstrate that at substoichiometric concentrations, mP-iA β_5 conjugates 4 delay A β_{40} fibril formation in a loading dependent manner.

Characterizations by ThT assays, AFM, and TEM show that mP-iA β_5 conjugates 4 not only modulate A β_{40} aggregation but also redirect from forming long, unbranched, one-dimensional fibrillar microstructures (Figure 2a) to the formation of zero-dimensional discrete nanostructures (Figure 2b–d and Figures S18, S23). When A β_{40} was incubated with 1.0 equiv of mP-iA β_5 conjugates 4, the ThT assays exhibited prolonged lag times, suggesting the lack of mature A β_{40} fibrils (Figure 2, left). These ThT results were confirmed by AFM and TEM studies (Figure 2, middle and right). More importantly, AFM and TEM studies demonstrated that A β_{40} incubated with 1.0 equiv of mP-iA β_5 conjugates 4 formed zero-dimensional discrete nanostructures at the end of the ThT experiments rather than the one-dimensional fibrils which were otherwise formed by A β_{40} control without any modulators. The AFM and TEM images show that discrete A β_{40} nanostructures stabilized by conjugates 4 have lateral dimensions ranging from 5 to 35 nm (Figure 2 middle and right, Figures S28, S29). When concentrations decreased to 0.5 equiv, mP-iA β_5 -7% 4 and mP-iA β_5 -12% 4 still stabilized A β_{40} into discrete nanostructures (Figures S18c', d', S23c', d'). However, mP-iA β_5 -3% 4 did not fully stabilize A β_{40} into discrete nanostructures at 0.5 equiv; instead, fibrils and nanostructures were both observed by AFM and TEM (Figures S18b', S23b'). Controls based on both polymer 5 and iA β_5 do not have the ability to redirect A β aggregation to form discrete nanostructures (Figures S15, S16, S24, and S25).

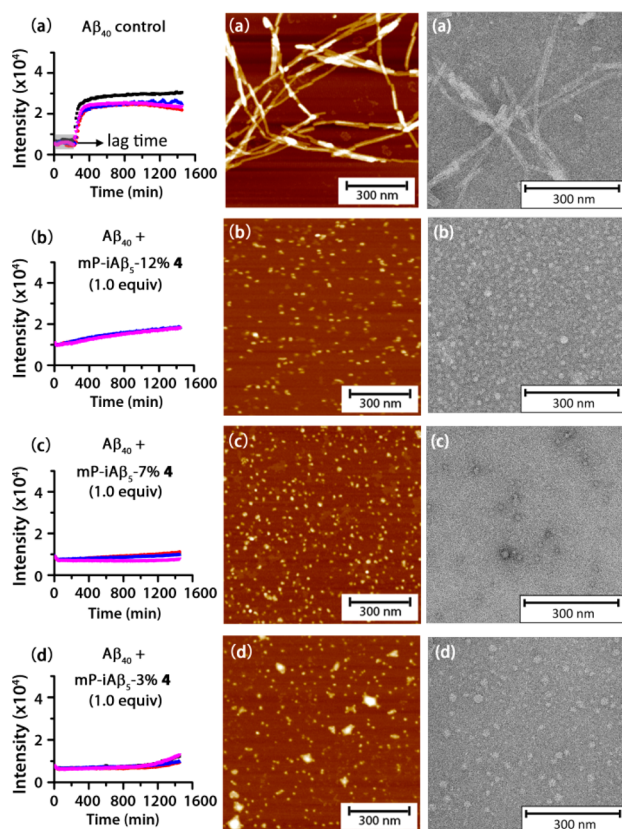


Figure 2. Effects of mP-iA β_5 conjugates 4 on A β_{40} aggregation monitored by ThT assays (left), AFM (middle), and TEM (right). (a) Kinetics of A β_{40} (15 μ M) aggregation was monitored by ThT assays without mP-iA β_5 conjugates 4. AFM and TEM images of A β_{40} (15 μ M) were recorded after incubation for 24 h in the absence of mP-iA β_5 conjugates 4. Kinetics of A β_{40} (15 μ M) aggregation was monitored by ThT assays with 1.0 equiv of mP-iA β_5 -12% 4 (b, left), mP-iA β_5 -7% 4 (c, left), and mP-iA β_5 -3% 4 (d, left). AFM and TEM images of A β_{40} (15 μ M) were recorded after incubation for 24 h with 1.0 equiv of mP-iA β_5 -12% 4 (b, middle and right), mP-iA β_5 -7% 4 (c, middle and right), and mP-iA β_5 -3% 4 (d, middle and right). Samples of AFM and TEM studies were taken directly from the ThT assays.

It is surprising that A β_{40} peptides self-assemble into discrete nanostructures in the presence of mP-iA β_5 conjugates 4. Although the composition of the discrete nanostructures has not been determined, we speculate that A β_{40} oligomers smaller than the critical-sized nucleus complex with conjugates 4 through multiple β -sheet interactions (Figure 3). These multivalent contacts prevent the A β nucleus from forming, and instead confine A β_{40} oligomers to a compact nanostructure, although we cannot exclude other possibilities such as interactions between A β_{40} monomers with conjugates 4 which initiate the formation of the discrete nanostructures.

In conclusion, we demonstrate that synthetic multivalent polymer–peptide conjugates are an effective strategy to noncovalently control fibrillar assembly of A β_{40} , a supramolecular polymerization governed by nucleation-dependent mechanism. It remains to be seen if this design concept is broadly applicable to the control of other nucleation-dependent supramolecular polymerizations. Our results show that mP-iA β_5 conjugates 4 modulate A β aggregation by redirecting the formation of A β fibrillar assemblies into discrete nanostructures. The composition of the nanostructures is currently under

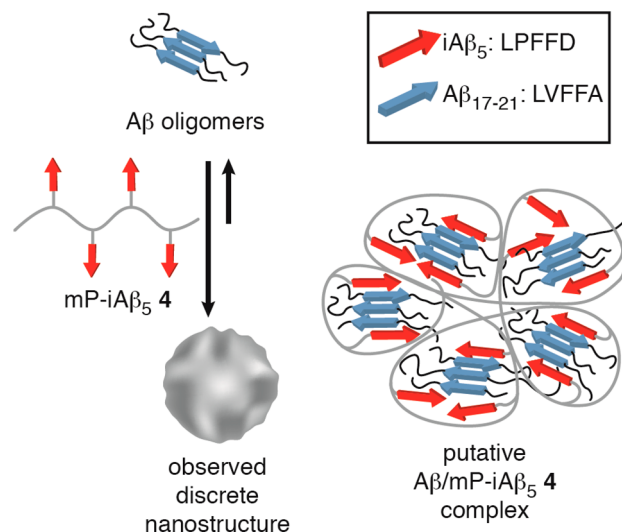


Figure 3. Hypothesis-based schematic representation of A β_{40} -derived nanostructure formation.

investigation and results of these studies will be published in due course.

■ ASSOCIATED CONTENT

Supporting Information

Details of synthesis of conjugates 4; ^1H NMR, GPC, FT-IR data of 3 and conjugates 4; ThT fluorescence assays, ATM and TEM studies of A β_{40} with iA β_5 , polymer 5, and conjugates 4; statistical size distribution based on TEM and DLS studies. This material is available free of charge via the Internet at <http://pubs.acs.org>.

■ AUTHOR INFORMATION

Corresponding Author

jsmoore@uiuc.edu

Notes

The authors declare no competing financial interest.

■ ACKNOWLEDGMENTS

We thank Prof. Boppart's group for allowing us to use their fluorescent plate reader. Research supported by the U.S. Department of Energy, Office of Basic Energy Sciences, Division of Materials Sciences and Engineering under Award No. DE-FG02-07ER46471.

■ REFERENCES

- (1) (a) Lomakin, A.; Chung, D.; Benedek, G.; Kirschner, D.; Teplow, D. *Proc. Natl. Acad. Sci. U.S.A.* **1996**, *93*, 1125–1129. (b) Cohen, S. I. A.; Linse, S.; Luheshi, L. M.; Hellstrand, E.; White, D. A.; Rajah, L.; Otzen, D. E.; Vendruscolo, M.; Dobson, C. M.; Knowles, T. P. J. *Proc. Natl. Acad. Sci. U.S.A.* **2013**, *110*, 9758–9763. (c) de Greef, T. F. A.; Meijer, E. W. *Nature* **2008**, *453*, 171–173. (d) Wang, R.; Liu, X.; Xiong, J.; Li, J. *J. Phys. Chem. B* **2006**, *110*, 7275–7280.
- (2) (a) Besenius, P.; Portale, G.; Bomans, P. H. H.; Janssen, H. M.; Palmans, A. R. A.; Meijer, E. W. *Proc. Natl. Acad. Sci. U.S.A.* **2010**, *107*, 17888–17893. (b) Hoshi, M.; Sato, M.; Matsumoto, S.; Noguchi, A.; Yasutake, K.; Yoshida, N.; Sato, K. *Proc. Natl. Acad. Sci. U.S.A.* **2003**, *100*, 6370–6375. (c) Bett, C. K.; Serem, W. K.; Fontenot, K. R.; Hammer, R. P.; Garno, J. C. *ACS Chem. Neurosci.* **2010**, *1*, 661–678. (d) Brambilla, D.; Verpillot, R.; Le Droumaguet, B.; Nicolas, J.; Taverna, M.; Kona, J.; Lettiero, B.; Hashemi, S. H.; De Kimpe, L.; Canovi, M.; Gobbi, M.; Nicolas, V.; Scheper, W.; Moghimi, S. M.;

Tvaroska, I.; Couvreur, P.; Andrieux, K. *ACS Nano* **2012**, *6*, 5897–5908.

(3) Zhao, D.; Moore, J. *Org. Biomol. Chem.* **2003**, *1*, 3471–3491.

(4) (a) Makin, O.; Atkins, E.; Sikorski, P.; Johansson, J.; Serpell, L. *Proc. Natl. Acad. Sci. U.S.A.* **2005**, *102*, 315–320. (b) FINDER, V. H.; Glockshuber, R. *Neurodegener. Dis.* **2007**, *4*, 13–27. (c) Colletier, J.-P.; Laganowsky, A.; Landau, M.; Zhao, M.; Soriaga, A. B.; Goldschmidt, L.; Flot, D.; Cascio, D.; Sawaya, M. R.; Eisenberg, D. *Proc. Natl. Acad. Sci. U.S.A.* **2011**, *108*, 16938–16943.

(5) (a) Soto, C.; Sigurdsson, E.; Morelli, L.; Kumar, R.; Castano, E.; Frangione, B. *Nat. Med.* **1998**, *4*, 822–826. (b) Soto, C.; Kindy, M.; Baumann, M.; Frangione, B. *Biochem. Biophys. Res. Commun.* **1996**, *226*, 672–680. (c) Viet, M. H.; Ngo, S. T.; Lam, N. S.; Li, M. S. J. *Phys. Chem. B* **2011**, *115*, 7433–7446.

(6) (a) Prokopova-Kubinova, S.; Vargova, L.; Tao, L.; Ulbrich, K.; Subr, V.; Sykova, E.; Nicholson, C. *Biophys. J.* **2001**, *80*, 542–548.

(b) Tucker, B.; Sumerlin, B. *Polym. Chem.* **2014**, *5*, 1566–1572.

(c) Duncan, R. *Nat. Rev. Drug Discovery* **2003**, *2*, 347–360.

(7) (a) Yanjarappa, M. J.; Gujraty, K. V.; Joshi, A.; Saraph, A.; Kane, R. S. *Biomacromolecules* **2006**, *7*, 1665–1670. (b) Perrier, S.; Takolpuckdee, P.; Mars, C. *Macromolecules* **2005**, *38*, 2033–2036.

(8) Godwin, A.; Hartenstein, M.; Muller, A.; Brocchini, S. *Angew. Chem., Int. Ed.* **2001**, *40*, 594–597.

(9) (a) Chafekar, S. M.; Malda, H.; Merckx, M.; Meijer, E. W.; Viertel, D.; Lashuel, H. A.; Baas, F.; Scheper, W. *ChemBioChem* **2007**, *8*, 1857–1864. (b) Cheng, P.-N.; Liu, C.; Zhao, M.; Eisenberg, D.; Nowick, J. S. *Nat. Chem.* **2012**, *4*, 927–933. (c) Cheng, P.-N.; Spencer, R.; Woods, R. J.; Glabe, C. G.; Nowick, J. S. *J. Am. Chem. Soc.* **2012**, *134*, 14179–14184.

(10) Krysmann, M. J.; Castelletto, V.; Kelarakis, A.; Hamley, I. W.; Hule, R. A.; Pochan, D. J. *Biochemistry* **2008**, *47*, 4597–4605.